Articles

Synthesis, Characterization, and Field-Effect Transistor Performance of Carboxylate-Functionalized Polythiophenes with Increased Air Stability

Amanda R. Murphy,[†] Jinsong Liu,[†] Christine Luscombe,[†] David Kavulak,[†] Jean M. J. Fréchet,*[,†] R. Joseph Kline,[‡] and Michael D. McGehee[‡]

Department of Chemistry, University of California, Berkeley, California 94720-1460, Material Science Division, Lawrence Berkeley National Laboratory, Berkeley, California 94720, and Department of Materials Science and Engineering, Stanford University, Stanford, California 94305-2205

Received April 29, 2005. Revised Manuscript Received July 20, 2005

Synthetic strategies to access both regiorandom and regioregular polythiophenes containing electron-withdrawing carboxylate substituents have been developed. Although these polymers have extended conjugation lengths, they provide better oxidative doping stability than conventional polythiophenes due to the lowering of the HOMO energy levels by approximately 0.5 eV. These materials are highly crystalline and exhibit very small $\pi-\pi$-stacking distances in the solid state. High charge mobilities are observed as a result of the close ordering of the polymer chains, and top-contact organic thin-film transistors (OTFTs) fabricated entirely in air had measured mobilities averaging 0.06 $cm^2/V\cdot s$ with on/off ratios $>10^5$. Off currents in these devices remained low over a period of months, demonstrating the low propensity of these materials toward p-doping by molecular oxygen.

Introduction

Organic semiconducting polymers have been the subject of intense study in recent years because they have shown potential as alternatives to inorganic semiconductors for low-cost optoelectronic devices, such as organic thin-film transistors[1−4] and photovoltaic cells.[5−9] Among these polymers, polythiophenes are the most commonly used due to their high charge carrier mobility. In particular, regioregular polythiophenes have shown the highest hole mobilities reported for any soluble polymeric system.[10−12] This high mobility is due in part to structural regularity, which leads to the formation of highly ordered lamella with cofacially stacked polymer backbones. The resulting small $\pi-\pi$-stacking distances (3.8 Å) enables efficient charge carrier hopping.[4,13]

A shortcoming associated with most commonly used organic semiconducting polymers is their sensitivity to air. This problem has been particularly noticeable when these materials are used as the active layer in organic thin-film transistors (OTFTs). It is generally believed that conjugated polymers are susceptible to p-type doping by interaction with ambient oxygen, resulting in larger off-currents and thus lower on/off ratios, as well as a positive shift in the threshold voltage for the transistor devices fabricated from these materials.[14,15] Therefore, when using polymer semiconductors such as poly(3-hexylthiophene) (P3HT), rigorous precautions must be taken during material processing and device fabrication to exclude environmental oxygen. These precautionary measures add to the cost of manufacturing, off-setting the appeal of polymer transistors as economical alternatives to silicon technology. Therefore, the development of semicon-

* Corresponding author. E-mail: frechet@berkeley.edu.
[†] University of California and Lawrence Berkeley National Laboratory.
[‡] Stanford University.

(1) Dimitrakopoulos, C. D.; Malenfant, P. R. L. *Adv. Mater.* **2002**, *14*, 99−117.
(2) Horowitz, G. *Adv. Mater.* **1998**, *10*, 365−377.
(3) Katz, H. E.; Bao, Z. N.; Gilat, S. L. *Acc. Chem. Res* **2001**, *34*, 359−369.
(4) Sirringhaus, H.; Tessler, N.; Friend, R. H. *Science* **1998**, *280*, 1741−1744.
(5) Brabec, C. J.; Sariciftci, N. S.; Hummelen, J. C. *Adv. Funct. Mater.* **2001**, *11*, 15−26.
(6) Coakley, K. M.; McGehee, M. D. *Appl. Phys. Lett.* **2003**, *83*, 3380−3382.
(7) Huynh, W. U.; Dittmer, J. J.; Alivisatos, A. P. *Science* **2002**, *295*, 2425−2427.
(8) Yu, G.; Gao, J.; Hummelen, J. C.; Wudl, F.; Heeger, A. J. *Science* **1995**, *270*, 1789−1791.
(9) Coakley, K. M.; McGehee, M. D. *Chem. Mater.* **2004**, *16*, 4533−4542.
(10) McCullough, R. D.; Williams, S. P. *J. Am. Chem. Soc.* **1993**, *115*, 11608−11609.
(11) Ong, B. S.; Wu, Y. L.; Liu, P.; Gardner, S. *J. Am. Chem. Soc.* **2004**, *126*, 3378−3379.
(12) Heeney, M.; Bailey, C.; Genevicius, K.; Shkunov, M.; Sparrowe, D.; Tierney, S.; McCulloch, I. *J. Am. Chem. Soc.* **2005**, *127*, 1078−1079.
(13) Sirringhaus, H.; Brown, P. J.; Friend, R. H.; Nielsen, M. M.; Bechgaard, K.; Langeveld-Voss, B. M. W.; Spiering, A. J. H.; Janssen, R. A. J.; Meijer, E. W.; Herwig, P.; de Leeuw, D. M. *Nature* **1999**, *401*, 685−688.
(14) Bao, Z. N.; Dodabalapur, A.; Lovinger, A. J. *Appl. Phys. Lett.* **1996**, *69*, 4108−4110.
(15) Meijer, E. J.; Detcheverry, C.; Baesjou, P. J.; van Veenendaal, E.; de Leeuw, D. M.; Klapwijk, T. M. *J. Appl. Phys.* **2003**, *93*, 4831−4835.

10.1021/cm050911d CCC: $30.25
Published on Web 09/02/2005

ducting polymers with high charge mobility as well as air stability is still needed.

The stability of organic semiconducting polymers toward oxidative doping is related to their ionization potentials, i.e., their highest occupied molecular orbital (HOMO) levels from vacuum. Therefore, lowering the HOMO energy level would improve environmental stability by minimizing the level of p-doping by ambient oxygen. This can be achieved by a number of methods, such as reducing the effective conjugation length to inhibit delocalization. Copolymers of thiophene with fluorene[16] have been shown to increase the air stability. Similarly, the incorporation of a thieno[2,3-*b*]thiophene[12] or a naphthalene unit[17] into the polymer backbone has been shown to afford greater environmental stability as well. Other research groups have taken the approach of increasing the rotational freedom of the backbone to reduce the π-overlap, which has also been an effective method for increasing stability.[11,18]

Another attractive method that has yet to be fully explored is to reduce the HOMO energy level of a semiconducting polymer through the incorporation of electron-withdrawing substituents. Most of the currently known polythiophene analogues contain either alkyl side chains or electron-donating substituents. Reports of polythiophenes with electron-withdrawing substituents are very few, presumably due to their difficult synthesis.[19,20] Polythiophenes with electron-withdrawing ester groups attached at the 3-position, namely poly(alkyl thiophene-3-carboxylates), have been synthesized by the Pomerantz group using the Ullmann coupling[21,22] or Kumada coupling reactions.[23] These polymers have shown high oxidation potentials due to the electron-withdrawing side chains, however, until now they have exhibited poor charge transport properties.

In this paper, we report new polythiophenes containing electron-withdrawing alkyl carboxylate substituents that exhibit high charge mobility. We have found that the regularity of the alkyl carboxylate substitution in our polythiophene can induce and facilitate molecular self-assembly in a fashion similar to that exhibited by regioregular P3HT[10] and poly(3,3‴-dialkylquaterthiophene)s (PQTs).[11] Due to the electron-withdrawing properties of the carboxylate substituents, our polymers have lower HOMO energy levels and therefore provide better oxidative doping stability than conventional solution-processible polythiophenes such as P3HT. Herein we describe the synthesis and characterization of these polymers in detail and report on their performance when used as the active layer in organic thin film transistors (OTFTs).

Scheme 1. Synthesis of the Regioregular Polythiophene 5 Functionalized with Dodecyl Carboxylates

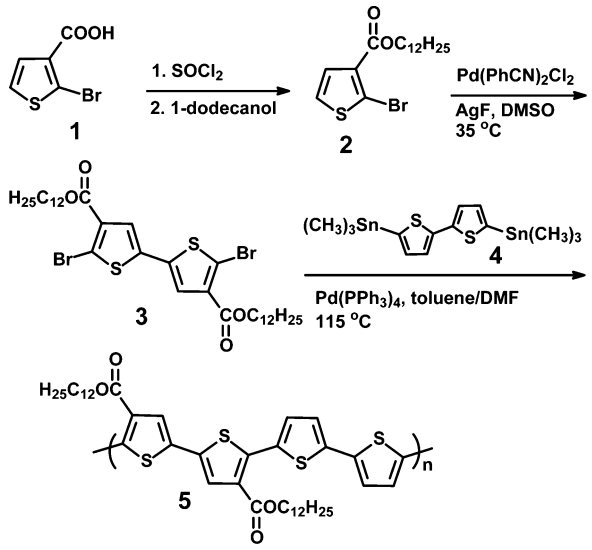

Results and Discussion

Synthesis. As shown in Scheme 1, an alternating copolymer of 2,2′-bithiophene and dialkyl 2,2′-bithiophene-4,4′-dicarboxylate was prepared, giving a regioregular, ester-functionalized polythiophene (**5**). Dodecyl 2-bromothiophene-3-carboxylate (**2**) was prepared using a modified literature procedure.[21,22,24] Compound **2** was transformed into didodecyl(5,5′-dibromo-2,2′-bithiophene-4,4′-dicarboxylate) (**3**) by an efficient palladium-catalyzed coupling reaction promoted by AgF, which was recently reported by the Mori group for the construction of symmetrical oligothiophenes.[25] The polymer was then synthesized via Stille-coupling polycondensation between **3** and 5,5′-di(trimethyltin) bithiophene (**4**) to produce **5** in high yield. This method for polymerization affords greater synthetic versatility than oxidative polymerization with $FeCl_3$,[11] allowing a variety of monomers to be copolymerized with **3**. This route also avoids the necessary dedoping and extensive removal of residual $FeCl_3$ from the polymer.[26]

The regioregularity of polymer **5** was analyzed using ^{1}H NMR (See Supporting Information). Only three types of aromatic protons can be seen in the spectrum, which confirms the structural symmetry and the regular arrangement of the side-chains in the polymer. Although polymer **5** has poor solubility in organic solvents at room temperature, it is very soluble in warm (>45 °C) chloroform, toluene, or 1,2-dichlorobenzene (*o*-DCB), which enables its solution processing. Size exclusion chromatography (SEC) data was obtained by first preparing a solution of the polymer in *o*-DCB and then diluting with THF. Calibration against polystyrene standards gave a number-average molecular

(16) Sirringhaus, H.; Wilson, R. J.; Friend, R. H.; Inbasekaran, M.; Wu, W.; Woo, E. P.; Grell, M.; Bradley, D. D. C. *Appl. Phys. Lett.* **2000**, *77*, 406−408.
(17) McCulloch, I.; Bailey, C.; Giles, M.; Heeney, M.; Love, I.; Shkunov, M.; Sparrowe, D.; Tierney, S. *Chem. Mater.* **2005**, *17*, 1381−1385.
(18) Ong, B.; Wu, Y. L.; Jiang, L.; Liu, P.; Murti, K. *Synth. Met.* **2004**, *142*, 49−52.
(19) Masuda, H.; Kaeriyama, K. *Makromol. Chem.-Rapid Commun.* **1992**, *13*, 461−465.
(20) Waltman, R. J.; Diaz, A. F.; Bargon, J. *J. Electrochem. Soc.* **1984**, *131*, 1452−1456.
(21) Pomerantz, M.; Yang, H.; Cheng, Y. *Macromolecules* **1995**, *28*, 5706−5708.
(22) Pomerantz, M.; Cheng, Y.; Kasim, R. K.; Elsenbaumer, R. L. *J. Mater. Chem.* **1999**, *9*, 2155−2163.
(23) Amarasekara, A. S.; Pomerantz, M. *Synthesis* **2003**, 2255−2258.
(24) Pomerantz, M.; Amarasekara, A. S.; Dias, H. V. R. *J. Org. Chem.* **2002**, *67*, 6931−6937.
(25) Masui, K.; Ikegami, H.; Mori, A. *J. Am. Chem. Soc.* **2004**, *126*, 5074−5075.
(26) Pomerantz, M.; Tseng, J. J.; Zhu, H.; Sproull, S. J.; Reynolds, J. R.; Uitz, R.; Arnott, H. J.; Haider, M. I. *Synth. Met.* **1991**, *41*, 825−830.

Scheme 2. Synthesis of the Regiorandom Alternating Copolymer 9

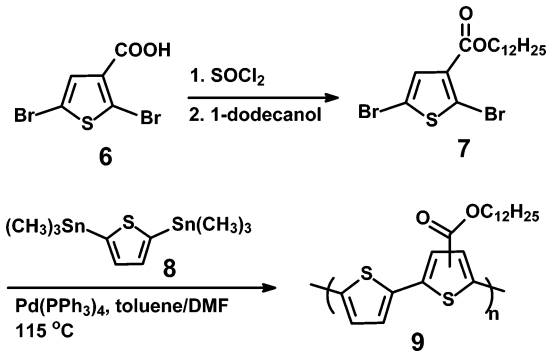

weight (M_n) of 6000 (M_w = 7500) with a polydispersity of 1.2. Similar molecular weights were measured using MALDI-TOF mass spectrometry.

The design of polymer **5** was based on several considerations: (1) The electron-withdrawing carboxylate side chains should increase the ionization potential of the polythiophene, (2) long alkyl (i.e. dodecyl) carboxylates are expected to enhance the solubility of the polymer, and (3) the side chains of the copolymer oriented symmetrically in the same direction in the extended polymer conformation are regularly spaced fairly far apart, similar to that of regioregular PQTs. This structural regularity coupled with the distance between adjacent alkyl chains should enable **5** to self-assemble and achieve intermolecular side-chain interdigitation in the condensed phase, therefore giving rise to three-dimensional lamellar π-stacking and high charge mobility.

For the purpose of comparison, a regiorandom alternating copolymer of thiophene and dodecyl thiophene-3-carboxylate (**9**) was also synthesized using an analogous synthetic approach (Scheme 2) described previously by our group.[27] The ^{1}H NMR of polymer **9** (See Supporting Information) displays five types of aromatic protons, which can be assigned to three types of regio-isomers (HH, HT, TT), confirming the regiorandom side chain distribution in the polymer. Polymer **9** also has poor solubility in common organic solvents at room temperature, but it is very soluble in warm solvents such as chloroform, toluene, and dichlorobenzene. SEC data was obtained in the same manner as used with polymer **5**, giving a number-average molecular weight of 4600 (M_w = 6600) with a polydispersity of 1.4.

UV−Vis Characterization. Absorption spectra of polymer **5** in *o*-DCB at various temperatures are displayed in Figure 1. At temperatures exceeding 50 °C, polymer **5** shows a single absorption band at 2.56 eV (λ_{max} ~ 489 nm). Below 50 °C, however, the low-energy vibronic bands, especially the lowest energy (0−0) band (617 nm), become more pronounced. This thermochromic transition at relatively high temperatures (~45 °C), suggests that the polymer has a very strong propensity for π-stacking. Similar spectral changes have been observed upon cooling solutions of neutral poly(3-alkylthiophenes).[28,29] Experimental and theoretical studies

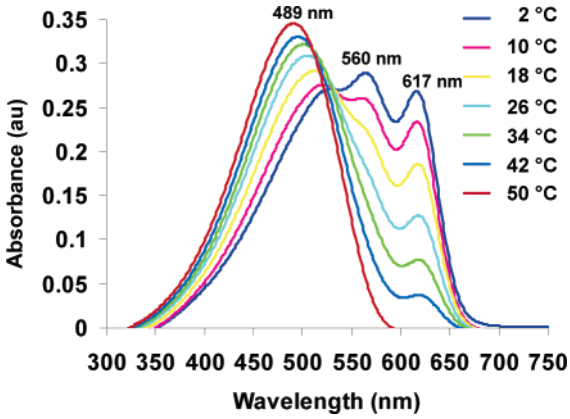

Figure 1. Solution UV−vis spectra of polymer **5** in *o*-DCB at various temperatures.

on various polythiophene derivatives and their related oligomers seem to indicate that such well-resolved red-shifted spectra obtained upon cooling correspond to π-stacked aggregated chain segments, which can originate from both inter- and intrachain stacking interactions.[30−33]

These low-energy vibronic states are also apparent in spun-cast films of polymer **5**, as shown in Figure 2a. This vibronic splitting, similar to that seen in other regioregular polythiophenes,[10,11] indicates the formation of highly ordered structures of lamellar π-stacked aggregates in the solid state. We found that the film processing conditions can significantly affect the solid-state absorption of polymer **5**. When cast from chloroform, the lowest-energy vibronic band (0−0) is about 2.07 eV (~600 nm). However, switching the casting solvent to *o*-DCB shifts this band to 2.0 eV (617 nm). Further annealing of this film at 100 °C increases the absorbance of the film and gives rise to an even more prominent lowest energy band in the spectrum. This significant bathochromic shift can be explained by the relative volatility of the casting solvents. Dichlorobenzene has a much lower volatility than chloroform, which provides a longer equilibration time for the self-assembly of the polymer chains and thus promotes better ordering within the film via π-stacking. The absorption bands for polymer **5** have a very large bathochromic shift when compared to those of the poly(alkyl thiophene-3-carboxylates) reported in the literature, indicating an increased conjugation length.[21,22]

Although polymer **9** shows a regiorandom conformation, as indicated by NMR, its absorption spectrum is similar to that of polymer **5**, as shown in Figure 2b. This observation is very different from the substantial absorption contrast between the regioregular poly(3-alkylthiophenes) and their regiorandom counterparts.[10] Presumably, as an alternating copolymer, polymer **9** can avoid direct head-to-head coupling, which would significantly disrupt the planar backbone

(27) Liu, J. S.; Kadnikova, E. N.; Liu, Y. X.; McGehee, M. D.; Fréchet, J. M. J. *J. Am. Chem. Soc.* **2004**, *126*, 9486−9487.
(28) Rughooputh, S. D. D. V.; Hotta, S.; Heeger, A. J.; Wudl, F. *J. Polym. Sci. B* **1987**, *25*, 1071−1078.
(29) Faid, K.; Frechette, M.; Ranger, M.; Mazerolle, L.; Levesque, I.; Leclerc, M.; Chen, T. A.; Rieke, R. D. *Chem. Mater.* **1995**, *7*, 1390−1396.
(30) Apperloo, J. J.; Janssen, R. A. J.; Malenfant, P. R. L.; Fréchet, J. M. J. *Macromolecules* **2000**, *33*, 7038−7043.
(31) Roux, C.; Bergeron, J. Y.; Leclerc, M. *Makromol. Chem.* **1993**, *194*, 869−877.
(32) Yang, C.; Orfino, F. P.; Holdcroft, S. *Macromolecules* **1996**, *29*, 6510−6517.
(33) Yue, S.; Berry, G. C.; McCullough, R. D. *Macromolecules* **1996**, *29*, 933−939.

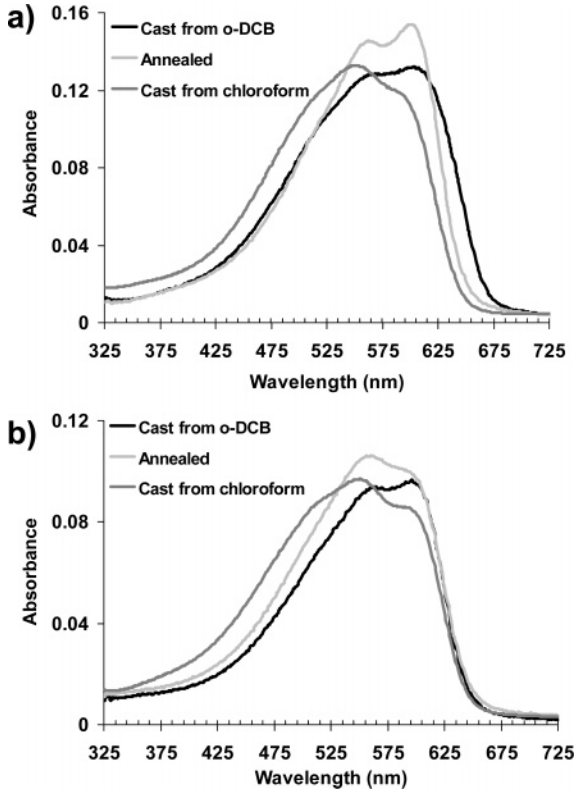

Figure 2. UV−vis spectra of films of polymers (a) **5** and (b) **9** cast from *o*-DCB and $CHCl_3$. Spectra from films cast from *o*-DCB then annealed at 100 °C are also given.

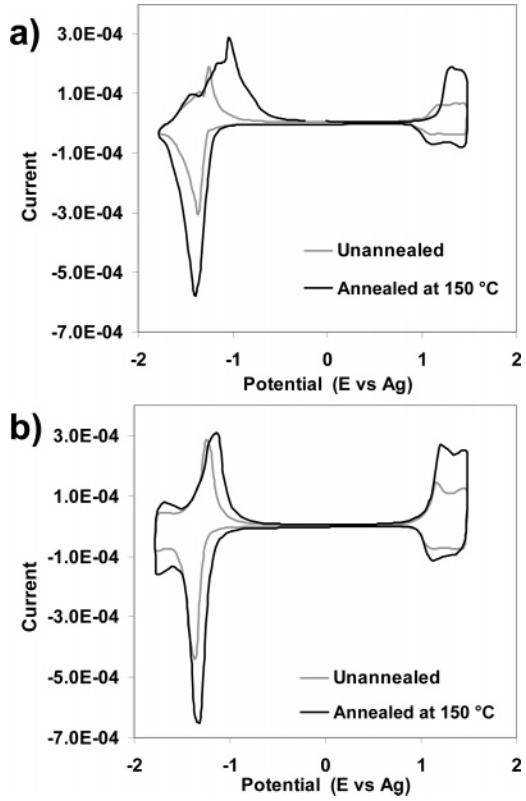

Figure 3. CV vs Ag of polymers (a) **5** and (b) **9** before and after annealing at 150 °C.

Table 1. Electrochemical Properties of Polymers 5 and 9 before and after Annealing at 150 °C as Compared to P3HT

	energy levels (eV)		
polymer	HOMO	LUMO	band gap (eV)
P3HT	−5.30	−2.95	2.35
5	−5.68	−3.47	2.21
annealed	−5.84	−3.49	2.35
9	−5.69	−3.47	2.23
annealed	−5.74	−3.54	2.20

conformation as observed in regiorandom poly(3-alkylthiophenes). Solid-state films of polymer **9** exhibited vibronic splitting similar to that of polymer **5**, suggesting that it is also likely to form ordered π-stacked aggregates. In contrast, when polymer **9** was drop-cast from *o*-DCB, its absorption spectrum did not exhibit a significant bathochromic shift from that of a film cast from chloroform (Figure 2b), as was observed for polymer **5**.

Cyclic Voltammetry. CV results (vs Ag/AgCl) are shown in Figure 3 for films made by dipping the working electrode in a solution of each polymer in *o*-DCB, before and after annealing at 150 °C. Both polymer **5** and **9** show good reversible scans (omitted for clarity) with small fluctuations in peak height stopping after the second cycle. Reversibility is seen for both oxidation and reduction reactions for both polymers, which demonstrates the electrochemical stability of the polymers even in their ionic states.

The HOMO and LUMO levels of the polymers can be estimated using this CV data. $E^{\mathrm{HOMO}} = -E^{\mathrm{ox}} - 4.4$ eV and $E^{\mathrm{LUMO}} = -E^{\mathrm{red}} - 4.4$ eV, where E^{ox} and E^{red} are the onset potentials of the oxidation and reduction peaks (vs SCE), respectively, and the 4.4 eV relates the SCE reference to vacuum.[34] Onset potentials were calculated as the intersections between two tangent lines extrapolated from the background baseline and the rising peak line.

As seen in Table 1, there is only a slight difference in energy levels between polymers **5** and **9** when the films are unannealed. These data support our hypothesis arising from the UV data that although polymer **9** is regiorandom, its alternating architecture prevents steric interactions between the alkyl chains and allows the polymer backbone to adopt a planar conformation. Upon annealing, polymer **5** exhibits a small decrease in the HOMO level by 0.14 eV, while the LUMO stays the same, resulting in an increase in the band gap to 2.35 eV. Polymer **9**, however, exhibits a small decrease in both the HOMO and LUMO levels upon annealing, leaving the band gap relatively unchanged.

Both polymers show band gap energies similar to that of P3HT, even though their energy levels are significantly lower. These data suggest that while electron-withdrawing groups added to conjugated polymer backbones do in fact lower HOMO and LUMO levels, both energy levels are affected by approximately the same magnitude. A lower HOMO level suggests that our new polymers should have a better oxidative stability than traditional P3HT.

DSC Analysis. Differential scanning calorimetry (heating at 5 °C/min) was employed to monitor any thermal transitions. As shown in Figure 4, both polymers have distinct endothermic transitions. The regioregular polymer **5** exhibits a rather broad melt to isotropic phase at 220 °C, and the

(34) Bredas, J. L.; Silbey, R.; Boudreaux, D. S.; Chance, R. R. *J. Am. Chem. Soc.* **1983**, *105*, 6555−6559.

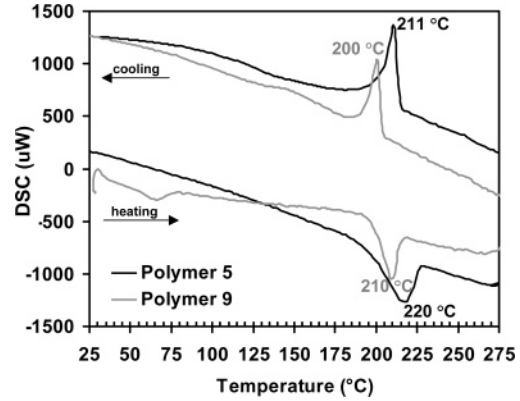

Figure 4. Differential scanning calorimetry of polymers **5** and **9** heating and cooling at 5 °C/min.

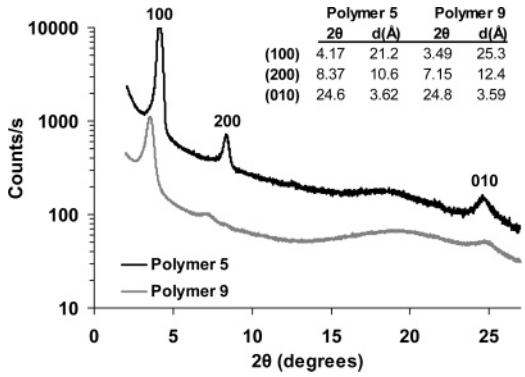

Figure 5. Thick film XRD analysis of polymers **5** and **9** deposited from *o*-DCB and annealed at 120 °C.

alternating copolymer **9** displays a sharper transition at 210 °C. Both polymers also show large exotherms upon cooling, where polymer **9** crystallizes 10 °C lower than polymer **5**. These endo- and exotherms are reversible over many cycles and are independent of the heating and cooling rate.

X-ray Diffraction (XRD) Analysis. To evaluate the crystallinity of polymers **5** and **9**, XRD measurements were taken of thick drop cast films that were annealed at 120 °C. As shown in Figure 5, polymer **5** exhibited distinct diffraction peaks at $2\theta = 4.17°$ and 8.37°, corresponding to an interchain lamellar *d*-spacing of 21.2 Å. A third peak at $2\theta = 24.6°$ corresponds to a $\pi-\pi$-stacking distance of 3.62 Å. This $\pi-\pi$-stacking distance falls in the region typically observed in regioregular polythiophenes (3.5−3.8 Å), and is 0.1 Å closer than the $\pi-\pi$-stacking distance observed in the structurally similar analogue PQT-12.[11] However, the interchain spacing between the individual polymer chains is higher than that observed in PQT-12. This increased spacing could be due to the ester functionality, which could force the alkyl chains to adopt a more vertical orientation. However, the precise orientation of the alkyl chains cannot be determined with XRD data alone, so further evaluation is needed to get an accurate view of the side chain conformations.

Polymer **9** exhibited much weaker diffraction peaks at $2\theta = 3.49°$ and 7.15°, corresponding to an interchain lamellar *d*-spacing of 25.3 Å. The third broad peak at $2\theta = 24.8°$ corresponds to a $\pi-\pi$-stacking distance of 3.59 Å. Even though this polymer is regiorandom, the polymer backbone remains very planar in the solid-state, resulting in a π-stacking distance comparable to that observed in the regioregular polymer **5**. This observation is also consistent with the UV−vis and CV data described above. However, the regiorandom nature of the side chains does manifest in a larger interchain lamellar distance.

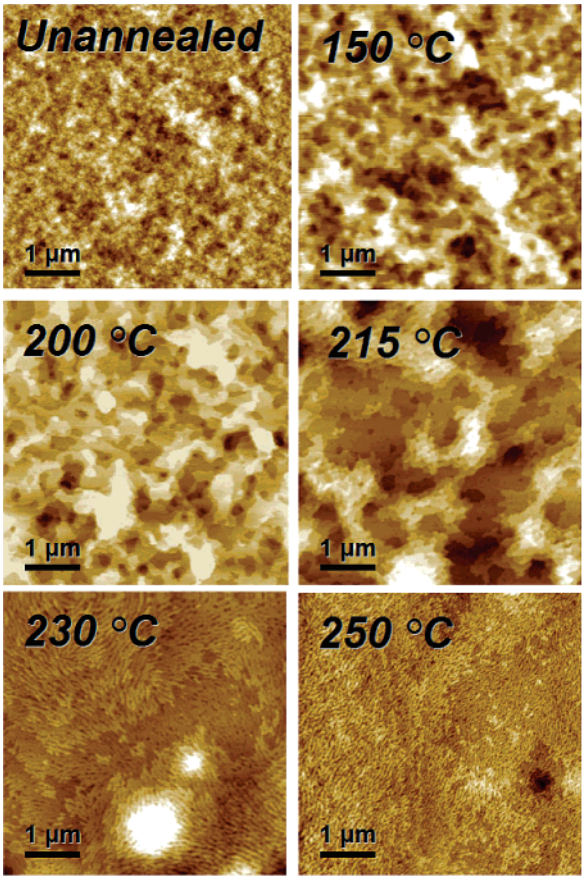

Figure 6. AFM images of films of polymer **5** on SiO_2 annealed for 20 min at the temperatures indicated and then cooled to room temperature.

AFM Film Imaging. The film morphology of both polymers was examined with AFM. Films were prepared by dissolving 2−3 mg/mL of polymer in *o*-DCB (heated to 80 °C) and then spin-casting at 1000 rpm on SiO_2 wafers. This film preparation method is analogous to that used below to construct the OTFT devices, thus enabling a correlation of the film morphology with the measured charge mobilities. To observe the effect of annealing on film topology, the films were annealed for 20 min at a range of temperatures both below and above the melting point observed in the DSC experiments. Controlling the rate of cooling of the samples did not produce significantly different morphologies; therefore, images presented here were taken from films cooled rapidly to room temperature. Also, no change in the AFM images was observed when the SiO_2 substrate was modified with octadecyltrichlorosilane (OTS), suggesting that the substrate does not influence the surface topology of the polymers.

The morphologies of the regioregular polymer **5** films annealed at different temperatures are shown in Figure 6. As cast, the films are relatively disordered but begin to smooth and order into π-stacked crystalline domains as the temperature increases to 200 °C. Above the melting point of 220 °C, a drastic change in morphology is seen with the

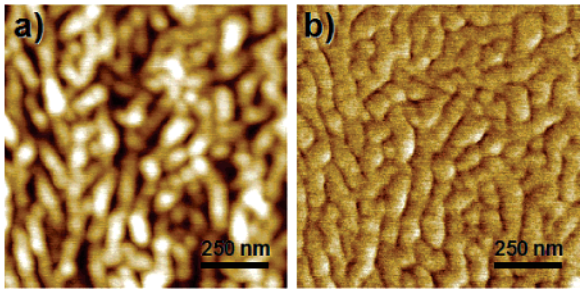

Figure 7. Higher resolution AFM (a) height and (b) phase image of polymer **5** annealed at 250 °C for 20 min.

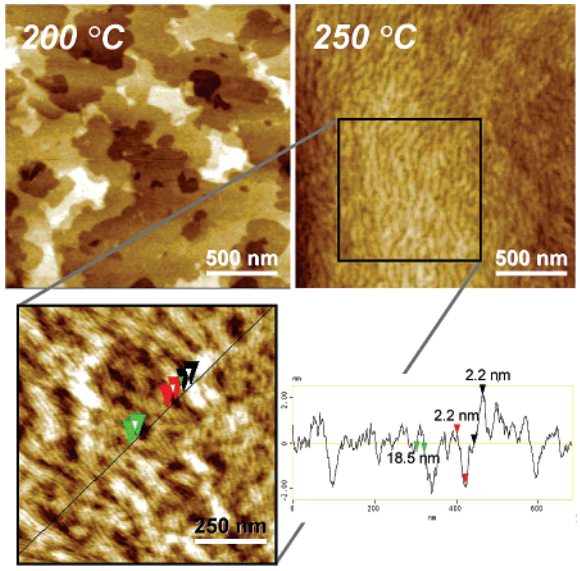

Figure 8. AFM images of polymer **9** annealed at the temperatures indicated. The lower image shows an enlarged height cross section of the film annealed at 250 °C.

appearance of rodlike crystalline domains. This type of morphology is similar to that seen when annealing PQT-12[35] or low molecular weight P3HT[36] and is indicative of the crystallization of highly ordered, cofacially π-stacked polymer backbones. A higher resolution scan of the film heated to 250 °C, shown in Figure 7, reveals that the width of these rods (~100 nm) is much larger than the expected length of the polymer calculated from the molecular weight (~10 repeat units = 13 nm). This suggests that the individual polymer chains are aggregating to form larger domains.

As seen in Figure 8, the alternating copolymer **9** gave rise to very similar morphology changes with temperature. Annealing at 200 °C produces relatively smooth crystal nodules, but heating above the melting point results in rodlike structures. The widths of the rods seen in this polymer are much smaller than that seen for polymer **5** and roughly correspond to the calculated length of a single polymer chain (~25 repeat units = 17 nm). Therefore, the regiorandom nature of this polymer results in the crystallization of long rods consisting of single polymer chain lamella rather than larger aggregates, as seen in the regioregular polymer **5**.

(35) Zhao, N.; Botton, G. A.; Zhu, S. P.; Duft, A.; Ong, B. S.; Wu, Y. L.; Liu, P. *Macromolecules* **2004**, *37*, 8307−8312.
(36) Kline, R. J.; McGehee, M. D.; Kadnikova, E. N.; Liu, J. S.; Fréchet, J. M. J. *Adv. Mater.* **2003**, *15*, 1519−1522.

Table 2. Average Hole Mobilities (μ) and on/off Ratios over 5−10 Devices for OTFTs Made with the Polymers Indicated[a]

	unannealed		150 °C		200 °C	
	μ ($cm^2/V\cdot s$)	on/off	μ ($cm^2/V\cdot s$)	on/off	μ ($cm^2/V\cdot s$)	on/off
			Polymer **5**			
bottom contact	0.0013	10^5	0.0077	10^6	0.0093	10^6
2 weeks in air	–		–		0.0069	10^5
4 months in air	–		–		0.0038	10^5
top contact						
untreated SiO_2	–		–		0.064	10^5
SiO_2 treated with OTS	0.0081	10^3	0.030	10^4	0.053	10^5
after 2 months in air	–		–		0.017	10^5
			Polymer **9**			
bottom contact	0.0004	10^4	0.0020	10^5	0.0032	10^6
4 months in air	–		–		0.0008	10^5
top contact						
untreated SiO_2	–		–		0.0040	10^3
SiO_2 treated with OTS	0.0009	10^2	0.0059	10^3	0.0063	10^4
2 months in air	–		–		0.0013	10^2
			P3HT			
top contact	0.0064	10^3				
after 1 week in air	0.0063	10				

[a] Regiorandom and regioregular polythiophenes containing electron-withdrawing carboxylate substituents were found to provide better oxidative doping stability than conventional polythiophenes, due to lower HOMO energy levels. Off currents in OTFT devices stored in air for months remained low, demonstrating the low propensity of these materials toward p-doping by molecular oxygen.

Electrical Characterization. OTFT devices were fabricated on low resistivity n-type silicon wafers, using thermally grown SiO_2 or SiO_2 treated with OTS as the dielectric, in bottom and top contact geometries. All device fabrication procedures were done in air. The active semiconducting layer was applied by spin-casting 2−3 mg/mL solutions in anhydrous *o*-DCB (heated to 80 °C) at 1000 rpm. The films were annealed at temperatures between 100 and 250 °C in air. For top contact devices, gold contacts were patterned on top of the films using various shadow masks, giving channel lengths from 5 to 40 μm and widths from 200 to 400 μm. Devices were tested in an ambient or nitrogen atmosphere as p-type OTFTs in the accumulation regime.

Table 2 lists the average hole mobilities and on/off ratios measured over 5−10 devices for both polymers under a variety of processing conditions and device geometries. The standard deviations in the mobility values were less than ±0.001, unless noted otherwise.

Maximum mobilities measured for polymer **9** in bottom contact devices were ~0.003 $cm^2/V\cdot s$ with on/off ratios ranging from 10^4 to 10^6. Top contact devices have slightly higher average mobilities of ~0.006 $cm^2/V\cdot s$ but with lower on/off ratios ranging from 10^3 to 10^4. Varying the processing conditions such as concentration and spin speed has very little effect on the mobility. Annealing the films at a temperature of 150 °C results in an order of magnitude increase in mobility and on/off ratio, but only slight increases are seen when the films are annealed above this temperature. Even though both of the polymers tested have similar conjugation lengths, energy levels, and morphology, in all cases the regioregular polymer **5** was found to have mobilities superior to thaose of polymer **9**. Decreased crystallinity as compared to polymer **5**, apparent in the XRD spectra, could be a cause for this diminished charge mobility.

Varying the processing conditions and device structure resulted in the same trends in charge mobility for the regioregular polymer **5**. As seen in Table 2, an increase in the average mobility from 0.0013 to 0.0077 $cm^2/V\cdot s$ can be achieved in bottom contact devices by annealing the sample at 150 °C prior to testing. Further increases are measured when the annealing temperature is increased to 200 °C, giving an average mobility of 0.0093 ± 0.002 $cm^2/V\cdot s$. This enhancement in mobility coincides with the formation of larger crystal domains observed upon annealing. Above the melting point of the polymer (not shown), an order of magnitude decrease in mobility is observed due to the formation of segregated rods consisting of $\pi-\pi$-stacked polymer lamella, which inhibit efficient charge transfer.[36,37] Mobility values can be pushed even higher by constructing top-contact geometry devices. Depositing the polymer on untreated SiO_2 or OTS-treated SiO_2 achieves similar results. Mobilities averaging 0.064 ± 0.02 and 0.053 ± 0.01 $cm^2/V\cdot s$, respectively, were measured when films were annealed at 200 °C. In all cases, devices routinely exhibited on/off ratios in excess of 10^5, demonstrating low propensity for doping by oxygen during the preparation of these devices in air.

The stability of the polymer devices stored in air was tested over time. Devices were stored in an ambient atmosphere, where they were not exclusively protected from light but did spend the majority of the time in the dark. As listed in Table 2, bottom contact devices exposed to air for up to 4 months showed a drop in mobility of ~60% for polymer **5** and ~75% for polymer **9**. In both cases, the on/off ratios lose an order of magnitude in the first weeks of exposure and then stay relatively constant at 10^5. Operation of these devices in air instead of nitrogen resulted in nearly identical threshold voltages, mobilities, and on/off ratios ranging from 10^5 to 10^6 (see Supporting Information). Top contact devices using OTS-treated SiO_2 faired similarly when exposed to air for up to 2 months. Polymer **5** exhibited a measured drop in mobility of ~70%, and polymer **9** decreased by ~80%. In this configuration, the on/off ratio stays constant at 10^5 for polymer **5** but decreases to 10^2 for polymer **9**. The origin of the drop in on/off ratio in this particular configuration has not been determined.

Transfer characteristics of OTFTs using polymer **5** as the semiconductor were monitored as a function of air exposure. Figure 9a,b illustrates that very low off currents are retained in bottom and top contact devices, even after months of exposure, confirming the oxidative stability of this polymer. Although the off current stays low in these devices, the saturation current decreases by about 75% in bottom contact devices (after 4 months) and about 40% in top contact devices (after 2 months). Also, large variations and an overall negative increase in threshold voltage (ranging from −10 to −25 V) were seen, particularly in the bottom contact devices, indicating a change in trap density within the films.[38] Changes in threshold voltage due to p-doping by oxygen

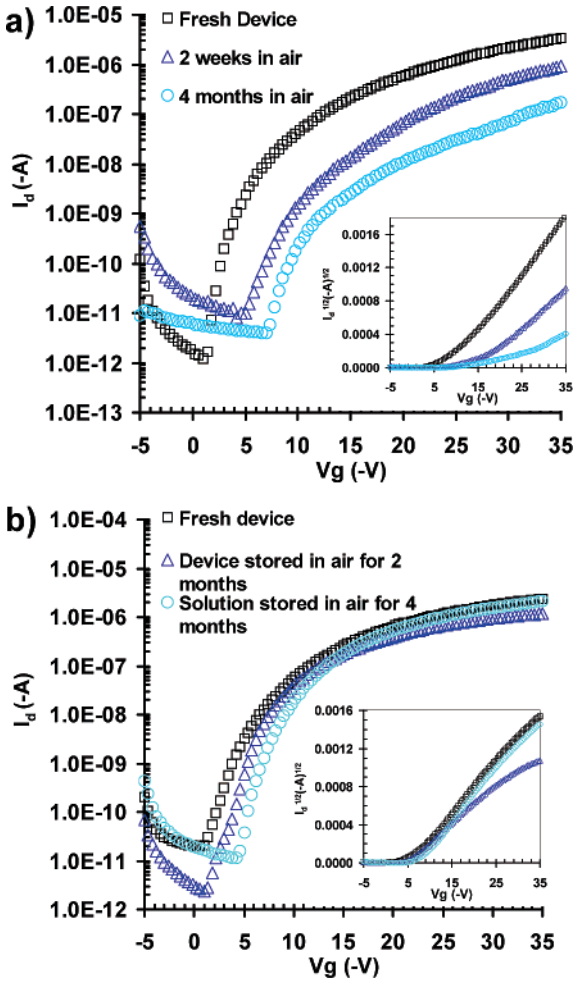

Figure 9. Transfer characteristics of devices made with polymer **5** as a function of time in the air. (a) V_g vs I_d (inset shows V_g vs $I_d^{1/2}$) for bottom contact devices with $L = 10$ μm and $W = 300$ μm at $V_d = -35$ V. (b) V_g vs I_d (inset shows V_g vs $I_d^{1/2}$) for top contact devices with $L = 40$ μm and $W = 400$ μm at $V_d = -35$ V.

shifts the threshold to positive voltages, but in this case a negative shift is observed. This type of behavior is difficult to interpret, and has previously been attributed to many effects, such as trapping at the dielectric-semiconductor interface,[39,40] the formation of bipolarons within the semiconductor,[41−43] or degradation of the semiconducting material. The transfer characteristics do not change upon repeated testing, indicating that a long-term stress effect is induced in the polymer rather than a transient bias effect. Reannealing the devices at 200 °C decreases the off current but does not reduce the threshold shift, ruling out moisture effects. Some recovery in the threshold voltage was seen when a positive bias was applied to the transistor (see Supporting Information) or after operating the device in white light, but the original threshold values could not be restored. Further investigation into the exact nature of this threshold shift is underway.

(37) Kline, R. J.; McGehee, M. D.; Kadnikova, E. N.; Liu, J. S.; Fréchet, J. M. J.; Toney, M. *Macromolecules* **2005**, *38*, 3312−3319.
(38) Brown, A. R.; Jarrett, C. P.; deLeeuw, D. M.; Matters, M. *Synth. Met.* **1997**, *88*, 37−55.
(39) Lin, Y. Y.; Gundlach, D. J.; Nelson, S. F.; Jackson, T. N. *IEEE Trans. Electron Devices* **1997**, *44*, 1325−1331.
(40) Torres, I.; Taylor, D. M.; Itoh, E. *Appl. Phys. Lett.* **2004**, *85*, 314−316.
(41) Salleo, A.; Street, R. A. *Phys. Rev. B* **2004**, *70*, 235324-1−235324-8.
(42) Salleo, A.; Street, R. A. *J. Appl. Phys.* **2003**, *94*, 471−479.
(43) Street, R. A.; Salleo, A.; Chabinyc, M. L. *Phys. Rev. B* **2003**, *68*, 085316-1−085316-2.

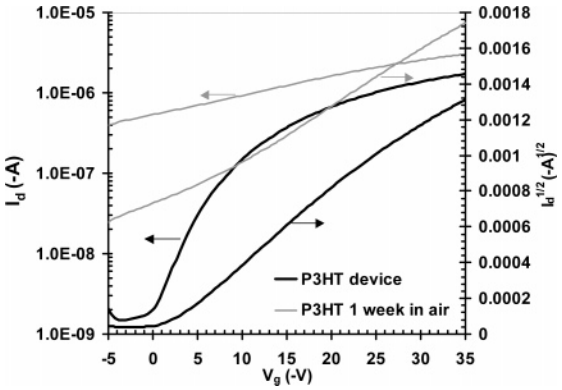

Figure 10. Transfer characteristics of a bottom-contact device of regioregular P3HT. Plots of V_g vs I_d and V_g vs $I_d^{1/2}$ for a device with $L = 20$ μm and $W = 400$ μm at $V_d = -35$ V.

Testing a solution of polymer **5** that had been made 4 months prior gave further confirmation of the stability. No precautions were taken to exclude oxygen during storage, and the solution was not fully protected from light. Top-contact device performance, shown in Figure 9b, was similar to those devices made with fresh polymer solutions. Charge mobilities up to 0.051 $cm^2/V\cdot s$ with on/off ratios of 10^5 were obtained.

Finally, devices were constructed using regioregular P3HT for comparison. Top contact devices were fabricated on untreated SiO_2, and the P3HT was deposited by spin-casting a 10 mg/mL solution in chloroform at 1000 rpm. All processing was done in the air. Initial testing of these devices produced mobility values of 0.006 $cm^2/V\cdot s$ with on/off ratios $\sim 10^3$. These devices were stored under the same conditions as the other polymers, but after only 1 week severe doping occurred where on/off ratios dropped to less than 10. Transfer characteristics of these devices are shown in Figure 10. While our new polythiophene analogue does show some long-term environmental effects, these effects are greatly reduced as compared to those of P3HT.

Conclusion

We have explored a new method for increasing the stability of polythiophenes toward oxidative doping by lowering the HOMO energy level through the addition of electron-withdrawing alkyl carboxylate substituents. The regioregular ester-functionalized polythiophenes were found to have high charge mobilities up to 0.07 $cm^2/V\cdot s$ with low off currents even when OTFT devices were fabricated entirely in air. This ability to tune the HOMO and LUMO levels of polythiophenes by introducing electron-withdrawing substituents while still maintaining good charge mobility will allow optimization of devices such as organic photovoltaics and sensors. These polymers are being utilized in ongoing projects in our laboratory to optimize the charge-transfer efficiency between the organic and inorganic phase in hybrid solar cell devices. These materials are also interesting candidates for organic sensors, since they are stable to the environment and possess interesting functional groups that may aid in their sensing ability.

Acknowledgment. We thank the AFOSR, DOE-BES (DE-AC03-76SF00098), and the National Science Foundation MRSEC Program for funding.

Supporting Information Available: Complete experimental procedures and characterization of **2**−**9** and ^{1}H NMR spectra of polymers **5** and **9**, as well as all OTFT fabrication procedures. This material is available free of charge via the Internet at http://pubs.acs.org.

CM050911D